Proceedings of the International Association for Shell and Spatial Structures (IASS) Symposium 2009, Valencia
Evolution and Trends in Design, Analysis and Construction of Shell and Spatial Structures
28 September - 2 October 2009, Universidad Politecnica de Valencia, Spain
Alberto DOMINGO and Carlos LAZARO (eds.)

One-DOF Cylindrical Deployable Structures with Rigid Quadrilateral Panels

Tomohiro TACHI*
* The University of Tokyo
7-3-1 Hongo , Bunkyo-ku, Tokyo 113-8656, Japan
ttachi@siggraph.org

Abstract

In this paper, we present a novel cylindrical deployable structure and variations of its design with the following characteristics:

1. Flat-foldable: The shape flattens into a compact 2D configuration.
2. Rigid-foldable: Each element does not deform throughout the transformation.
3. One-DOF: The mechanism has exactly one degree of freedom.
4. Thick: Facets can be substituted with thick or multilayered panels without introducing the distortion of elements.

Keywords: origami, deployable structure, flat-foldable, rigid-foldable, isometric transformation

1 Introduction

Cylindrical deployable and collapsible structures composed of two-dimensional elements are useful in various designs. Such a structure can form a watertight surface that encloses a certain desired volume by the addition of two surfaces at the ends, and the surfaces can be compactly folded down into a two-dimensional state. Several flat-foldable cylindrical deployable structures have been proposed thus far, e.g., by Hoberman [3], Guest and Pellegrino [1], Sogame and Furuya [7], and Nojima [6]. However, all of these existing deployable tubes are bistable structures whose transformation mechanisms rely on the in-plane elastic deformation. Since the mechanism of such a structure relies on the material flexibility, the applications were limited: e.g., an energy absorption device that can be used only once, as proposed by Wu *et al.* [8], a small-scale medical device by Kuribayashi *et al.* [4], a deployable membrane structure for use in space proposed by Sogame and Furuya [7].

In this paper, we propose cylindrical deployable structures in which every element of the surface is geometrically free of distortion. This enables the construction of mechanisms using

stiff materials, and such mechanisms can potentially be applied to designing repeatedly foldable architectural or human-scale structures under gravity. We first introduce the basic unit structure, and then, we generalize it to obtain isotropic and anisotropic types of structures, both of which produce one-DOF rigid motions. Furthermore, we present methods for realizing an isotropic type of generalized mechanism with thick panels and piano hinges and for realizing an anisotropic mechanism with multilayered thin surfaces.

2 Basic Geometry

The basic unit structure is constructed by joining two pieces: a single vertex origami with four congruent parallelograms and its mirror image (with respect to the zx-plane), as shown in Figure 1(a). The same structure is also known in the field of artistic origami, where Thoki Yenn designed a model "Flip Flop" by combining two units [9]. The vertex produces a one-DOF transformation mechanism in which the edges on the plane of reflection (zx-plane) always lie on the plane. This enables the formation of a valid joint structure from two pieces. The rhombus at each end, which we call the "section rhombus," is maintained co-planar (parallel to xy-plane) throughout the transformation. This enables the repetition of the units in the axial direction (z direction), to construct a cylinder of arbitrary length (Figure 2).

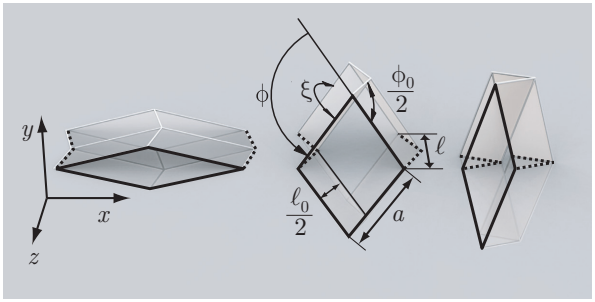

(a) Mechanism of the unit. Note that four edges on the plane of reflection (dotted lines) are kept on the plane while the section rhombus (solid lines) is kept coplanar.

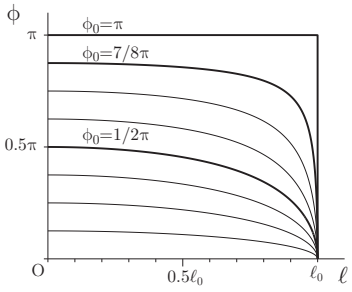

(b) The relation between ℓ and ϕ

Figure 1: Motion of a single unit.

The structure transforms from the completely unfolded state to the flat-folded state. In the flat-folded state, the distance between two adjacent units is zero. This means that a long cylindrical structure with multiple units can be compactly folded in the axial direction. We will now investigate the relationship between the folding motion in the axial direction and the deformation of the section rhombus. Let ξ and ϕ denote the dihedral angle between facets incident to the edge of the section rhombus (all four dihedral angles are equal) and the external angle of the top vertex of the section rhombus, respectively, as shown in Figure 1(a).

These two angles are related as follows:

$$\tan\frac{\phi}{2}\cot\frac{\phi_0}{2}=\cos\frac{\xi}{2}, \tag{1}$$

where $\phi_0(0<\phi_0<\pi)$ is the angle ϕ when the model is flat-folded. The distance ℓ between adjacent units is written in terms of ϕ as

$$\ell=\sqrt{1-\tan^2\frac{\phi}{2}\cot^2\frac{\phi_0}{2}}\ell_0, \tag{2}$$

where ℓ_0 is the distance in the unfolded state. As shown in Figure 1(b), ϕ_0 is the key parameter that controls the relation between two motions. When ϕ_0 is close to π a strongly non-linear motion approximated by a series of two separate motions is produced. We assumed that $\phi_0\neq\pi$, because for $\phi_0=\pi$, the folding motions of the units are completely independent of each other.

The unit occupies a volume of $a^2\ell\sin\phi$, where a indicates the length of each side of the rhombus. The volume is zero in the unfolded and flat-folded states, and it attains the maximum value $\sqrt{\frac{1}{1+2\cot^2\frac{\phi_0}{2}}}\ell_0a^2$ at $\cos\phi=\frac{1+\cos\phi_0}{2}$. The maximum volume increases as ϕ_0 approaches π.

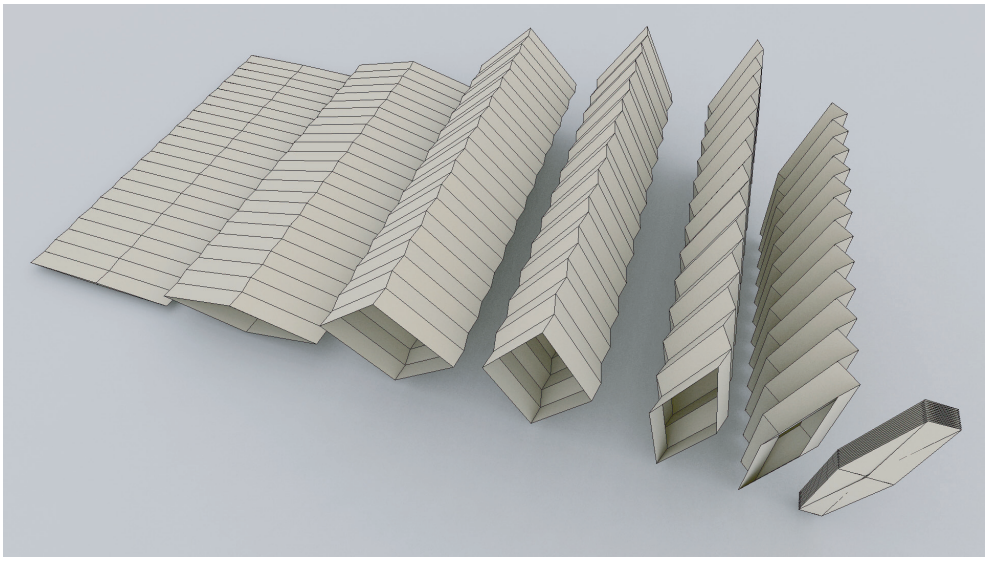

Figure 2: A rigid-foldable cylindrical structure with ϕ_0 close to π ($\phi_0=168°$).

3 Generalizations

Rigid-foldability of the proposed structure can be interpreted in two different ways, each of which results in a different method of generalization: “isotropic generalization” or “anisotropic

generalization."

3.1 Isotropic Generalization

The first interpretation is that the unit is composed of mechanical joints, which we call "folds" and "elbows." The joints are constructed by reflecting a two-facet strip with a V-shaped section with respect to a plane perpendicular to the bisector plane of the dihedral angle; the fold is constructed by ray reflection, while the elbow is constructed by image reflection (Figure 3(a)). We call these vertices isotropic because in these special cases of vertices, the absolute values of dihedral angles for incidence on opposite edges are equal.

We model the unit of a cylinder by connecting these joints to form a closed linkage. The bisector planes of dihedral angles are set on the common section plane. The polygonal linkage changes its shape within the plane according to the common dihedral angle ξ. This generally prevents a unit from being rigid-foldable, i.e., changing the ξ of a cylindrical shape can result in its edges tearing, as shown in Figure 4. Our goal is to ensure that the loops are always valid for any value of ξ.

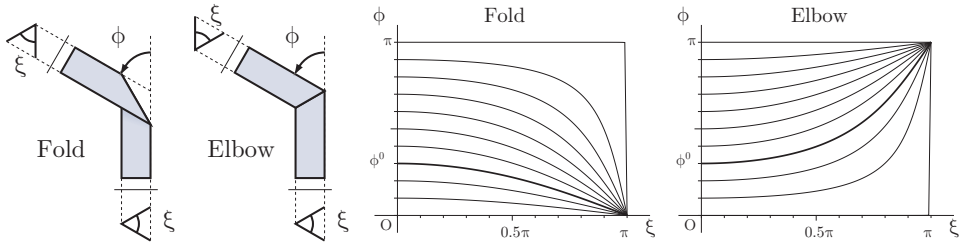

(a) Fold and Elbow (b) Relationship between ξ and ϕ

Figure 3: Fold and Elbow

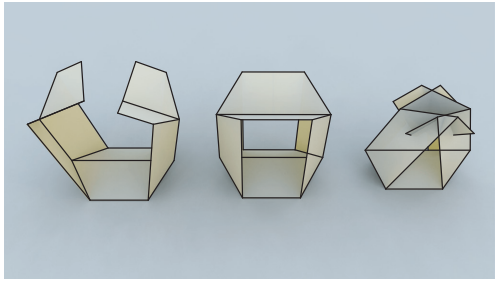

Figure 4: Unfolding (Left) or folding (Right) results in breaking the valid loop.

A joint enables a one-DOF mechanism that converts motion in the axial direction to motion in the section plane, which are represented by angles ξ and ϕ, respectively (Figure 3(a)). In

the same manner as Equation (1), the conversion from ξ to ϕ can be determined in terms of a parameter ϕ_0, the angle ϕ in the flat-folded state (Figure 3(b)).

$$\phi^{\text{fold}}(\phi_0, \xi) = 2\arctan\left(\cos\frac{\xi}{2}\tan\frac{\phi_0}{2}\right) \tag{3}$$

$$\phi^{\text{elbow}}(\phi_0, \xi) = \begin{cases} 2\arctan\left(\sec\frac{\xi}{2}\tan\frac{\phi_0}{2}\right) & \text{if } \xi \neq \pi \\ \pi & \text{if } \xi = \pi. \end{cases} \tag{4}$$

We can construct a valid loop by first constructing a half-loop linkage whose end edges remain parallel for any ξ and then connecting the linkage with its copy rotated by 180 degrees. The half loop must satisfy the following equation for any ξ ($0 \leq \xi \leq \pi$):

$$\sum_{\text{all folds}} \phi^{\text{fold}}(\phi_0, \xi) + \sum_{\text{all elbows}} \phi^{\text{elbow}}(\phi_0, \xi) = \pi. \tag{5}$$

In order to obtain such a half-loop, we use the following three combinations that make their sums constant:

$$\phi^{\text{fold}}(\phi_0, \xi) + \phi^{\text{fold}}(-\phi_0, \xi) \equiv 0, \tag{6}$$

$$\phi^{\text{elbow}}(\phi_0, \xi) + \phi^{\text{elbow}}(-\phi_0, \xi) \equiv 0, \tag{7}$$

$$\phi^{\text{fold}}(\phi_0, \xi) + \phi^{\text{elbow}}(\pi - \phi_0, \xi) \equiv \pi. \tag{8}$$

These three pairs can be seen as the fundamental pairs of joints required to construct a valid linkage. Connecting these pairs of joints in an arbitrary ordering such that the sum of the angles is π results in a valid half-loop linkage. The sequence in the basic structure is constructed using Equation (8) and can be represented as follows:

$$\mathrm{f}(\phi_0)\mathrm{e}(\pi - \phi_0),$$

where $\mathrm{e}(\phi_0)$ and $\mathrm{f}(\phi_0)$ represent an elbow and a fold, respectively. Figure 5 shows an example of the isotropic generalization realized by using this method. The sequence of joints in this example (half-loop from the bottom facet to the top facet in the counterclockwise direction) is,

$$\mathrm{f}(\tfrac{7\pi}{8})\mathrm{f}(-\tfrac{3\pi}{4})\mathrm{f}(\tfrac{3\pi}{4})\mathrm{f}(-\tfrac{3\pi}{4})\mathrm{f}(\tfrac{3\pi}{4})\mathrm{e}(\tfrac{\pi}{8})\mathrm{f}(-\tfrac{7\pi}{8})\mathrm{f}(\tfrac{3\pi}{4})\mathrm{f}(-\tfrac{3\pi}{4})\mathrm{f}(\tfrac{3\pi}{4})\mathrm{f}(-\tfrac{3\pi}{4})\mathrm{f}(\tfrac{7\pi}{8}).$$

In this example, the substructures based on Miura-ori, $\mathrm{f}(-\frac{3\pi}{4})\mathrm{f}(\frac{3\pi}{4})$, are inserted in order to make the model expand in the radial directions as well as in the axial direction.

3.2 Anisotropic Generalization

The proposed structure is a collection of parallelogram strips —in each strip, it is ensured that the edges between facets are parallel. We can construct a general valid cylindrical structure based on the parallelogram strips in the following manner. First, draw an arbitrary closed polyline with two-fold rotational symmetry, i.e., a zonogon, on the section plane; the zonogon represents a shape of the section. We call this zonogon a "section zonogon." Then, extrude

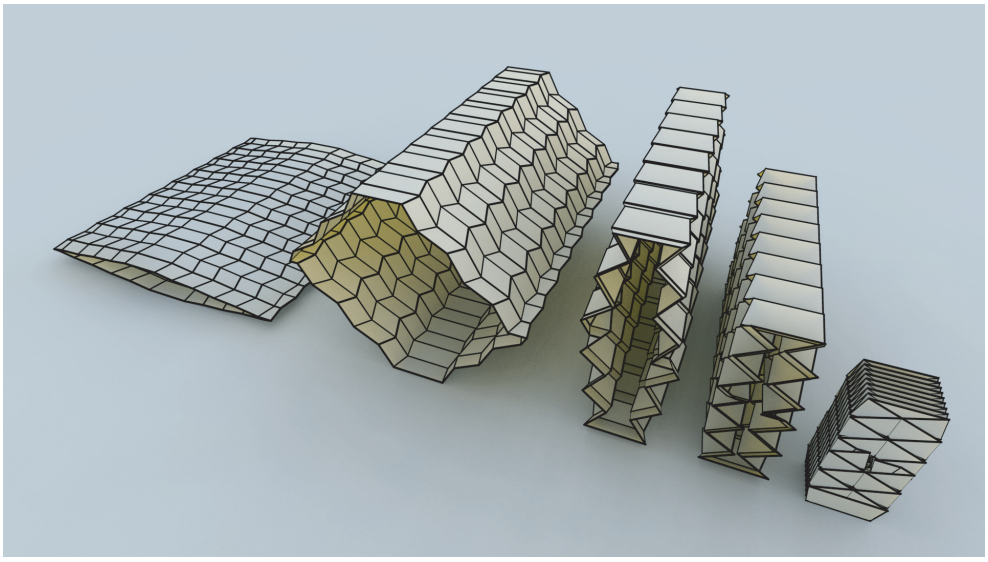

Figure 5: An isotropic generalization with radial expansive motion.

the section zonogon along an arbitrary vector at an angle of $\frac{\xi_0}{2}$ to the section plane in order to from a closed parallelogram strip. Without loss of generality, we assume that this vector, which we call the "extrusion vector," is parallel to the zx plane; the extrusion vector is represented as $\mathbf{l}_0 = \left(\ell \cos\frac{\xi_0}{2}, 0, -\ell \sin\frac{\xi_0}{2}\right)$, where ℓ is the length of the vector. Next, connect the strip to its mirror image with respect to the extruded section plane. Thus, we obtain the single unit.

The valid motion of the structure is produced as follows. We pick up half of the parallelogram strip and fold it along its edges. It is ensured that the edges, i.e., the extruded vertices, remain parallel after the folding. The direction of the edges is represented as a rotated extrusion vector $\mathbf{l} = \left(\ell \cos\frac{\xi}{2}, 0, -\ell \sin\frac{\xi}{2}\right)$. On the other hand, the section zonogon must lie on the section plane throughout the transformation. These constraints determine the orientation of each facet, and thus, they determine the orientation of each side of the section zonogon, independently with respect to the rotation of adjacent facets. Assume that a side of the section zonogon forms an angle θ with the x axis. Thus, it is represented as a vector $\mathbf{r} = (r\cos\theta, r\sin\theta, 0)$, where r is the length of the segment (Figure 6). The vector $\mathbf{r}$ is rotated such that the angle between the edge and the extrusion vector is constant, i.e., $\mathbf{l} \cdot \mathbf{r} = \text{const}$. Hence, we obtain the following relation:

$$\cos\theta = \frac{\cos\frac{\xi_0}{2}}{\cos\frac{\xi}{2}} \cos\theta_0,$$

where $\theta_0 = \theta|_{\xi=\xi_0}$. The sign of θ is determined by the sign of θ_0. If $\theta_0 = 0$, the facet can be rotated in both directions. Now, we have obtained the folded half-strip. The other half of

the strip is folded in the same manner and the corresponding end edges of the half strips meet because they are parallel and equal in length.

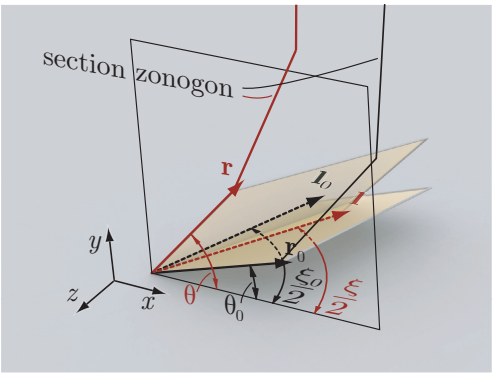

Figure 6: Rotation of a parallelogram.

The generalized structure is collapsible: the flat-folded state corresponds to the case where the half-strip is completely flattened. However, unlike the isotropic generalized structures, the completely unfolded state does not commonly exist. This is because the extrusion of an arbitrary polyline produces anisotropic vertices, in which the two dihedral angles of the opposite edges are not equal. The unfolding motion from the flat-folded state stops when any of the sides become horizontal i.e., $\cos\theta = 1$. Figure 7 shows an example of the generalized form.

4 Realization of Thick Surface

For the structure described in the previous sections, it was assumed that the thickness of the material is zero. However, in a real engineering application, the surface must be realized using a material with non-negligible thickness. In particular, in an architectural context, it is necessary to design structures with rigid panels or multilayered surfaces with a desired thickness. We propose two methods to realize the desired thickness without the loss of rigid-foldability: a method in which facets and foldlines are replaced with thick panels and piano hinges, respectively, and a method that enables thick multilayed surfaces composed of surfaces of negligible thickness. The former can be applied to the isotropic generalization and the latter to the anisotropic generalization.

4.1 Thick Panels

The basic structure (Section 2) and its isotropic generalization (Section 3.1) can be realized by using thick panels and rotating hinges (Figure 8). In order to avoid the interference that occurs when folding thick panels, we shift each axis of rotation to the side of the mountain fold, as shown in Figure 9(a). The structures of the vertices are changed in order to account for the point of intersection of the shifted axes, which are no longer coincident. In general, a vertex with non-concurrent incident axes yields 6 constraints, as opposed to a concurrent

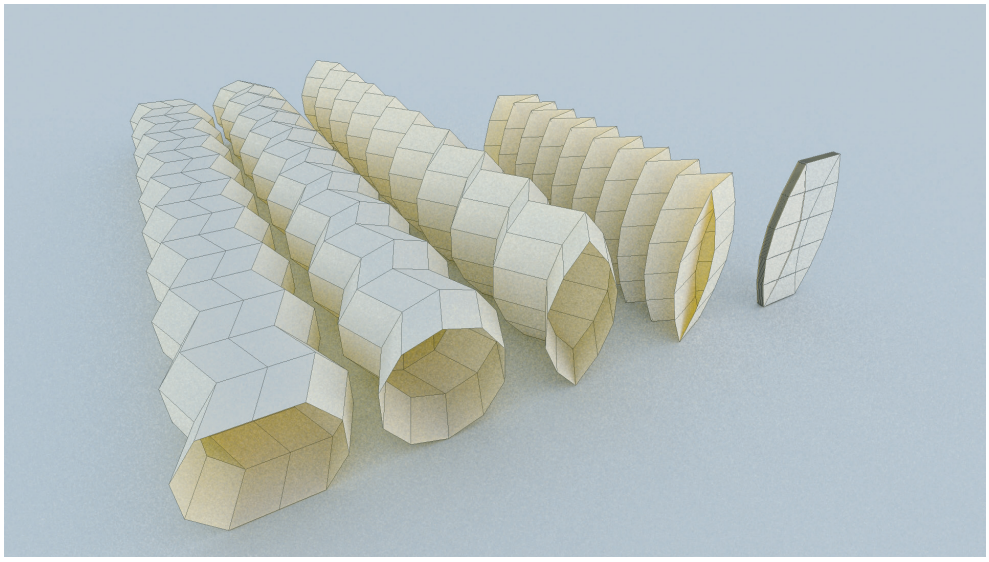

Figure 7: Folding motion in an example of anisotropic generalization. Only the top facets are flat in the most unfolded state (Left).

origami vertex with 3 constraints; this means that a general degree-4 vertex can become an overconstrained structure.

In order to realize a valid mechanism without overconstraints, we utilize special rigid body joints that replace the folds and the elbows. There are three types of mechanisms, as shown in Figure 9(b): one for the fold and two for the concave and convex elbows. A fold joint is replaced by panels with two thicknesses; in order to achieve valid motion, the thickness of the connection part in the fold joint is set as a half of the thickness in the other parts. The same idea is used by Hoberman [2], who realizes deployment mechanisms based on thick origami. A concave elbow (an elbow with a negative gauss area) and a convex elbow (an elbow with a positive gauss area) can be replaced with panels of constant thickness.

4.2 Multilayering

An anisotropic structure based on parallelogram strips can be realized using multilayered surfaces. As discussed in Section 3.2, each edge of the zonogon is uniquely assigned a valid orientation for a given folding angle $\frac{\xi}{2}$ of the extrusion vector. This enables a connected cylindrical structure extruded from multiple zonogons sharing a vertex and edges to transform without being separated. Hence, a composite structure of rigid-foldable and flat-foldable multilayered cylindrical structures is obtained by tessellating the original section zonogon with multiple zonogonal tiles (Figure 10). We can control the composition of the layers by changing the size of tiles or by subdividing the parallelograms.

This multilayering method also yields various designs with arbitrary composite sections. Figure 11 shows an example of a flat-foldable and rigid-foldable multilayered single curved sur-

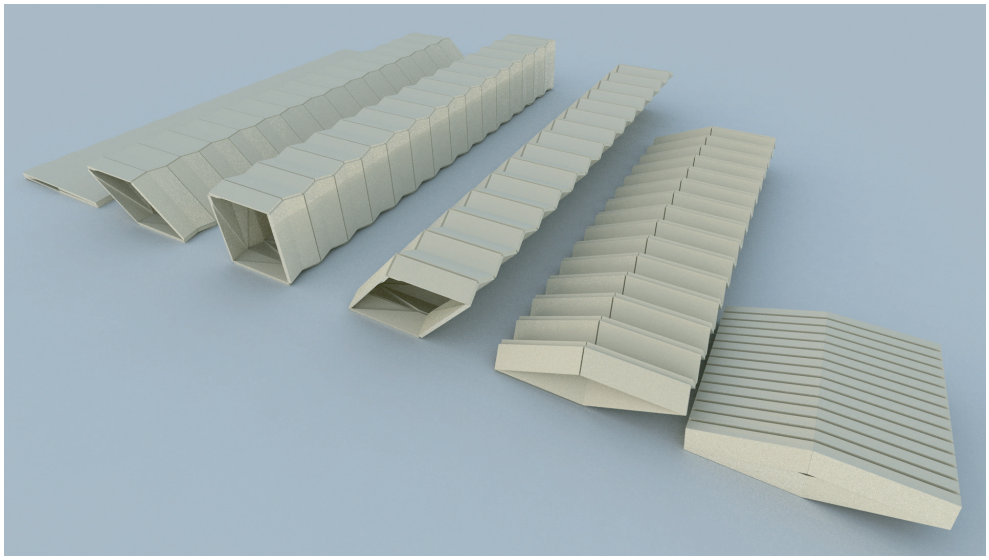

Figure 8: Folding motion of the structure with thick panels. The axes of rotation lie on the edges of the thick panels.

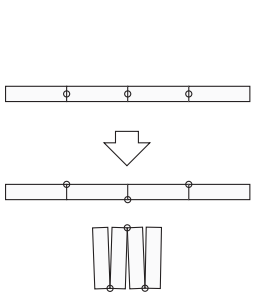

(a) The shifting of the axes.

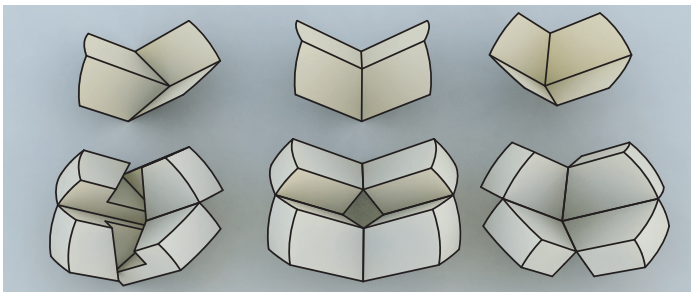

(b) Rigid body structure with non-concurrent axes replacing the joints. Left: Fold joint. Middle: Concave elbow. Right: Convex elbow.

Figure 9: Realization with thick panels and hinges.

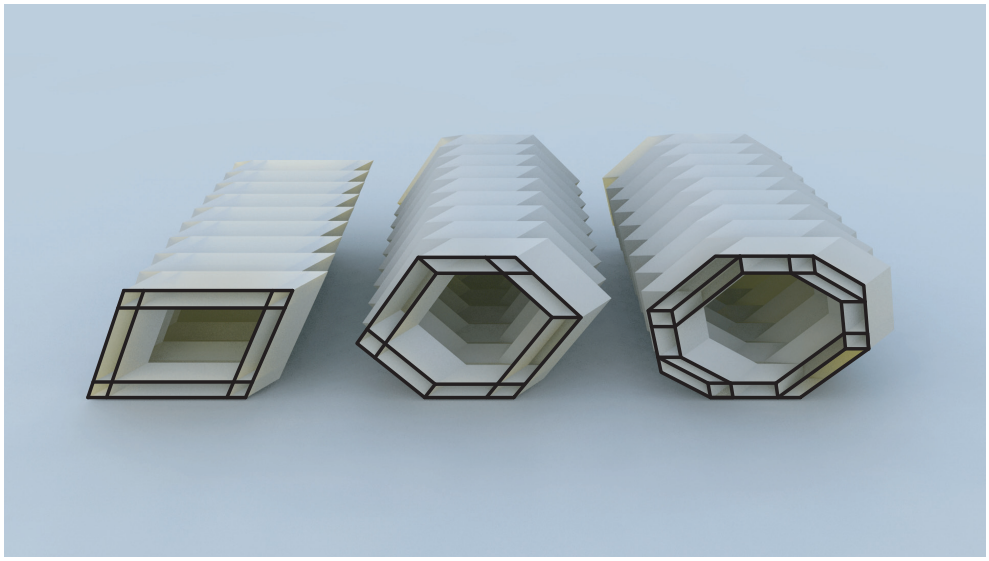

Figure 10: Multilayered cylinders. The section is composed of zonogons.

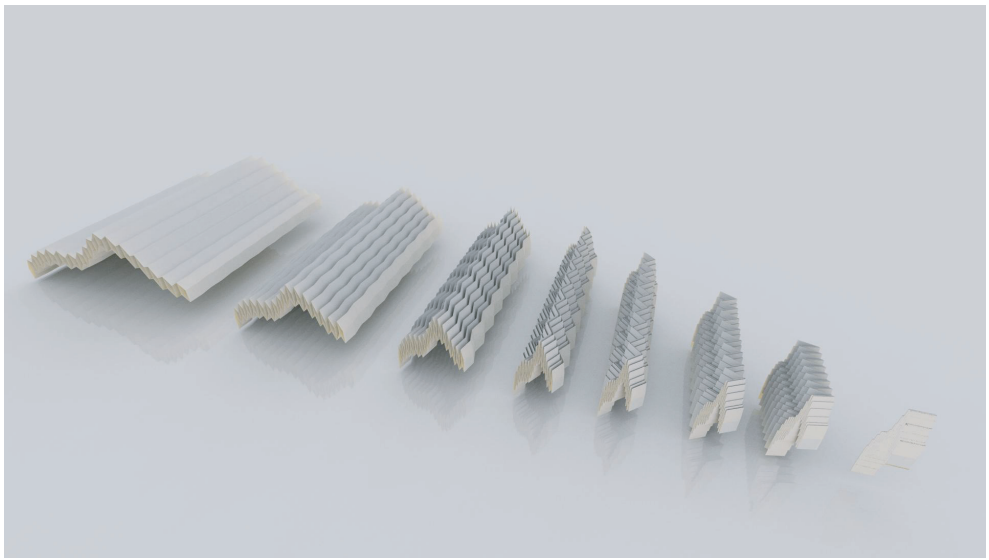

Figure 11: The folding motion of a multilayered surface along a given two-dimensional curve.

face. The structure is automatically constructed such that the section is formed by connected parallelograms along a given two-dimensional curve. In order to make the flat-folded shape compact, we use an evenly spaced zigzag polyline. We have implemented a parametric design of this type of structure using *Grasshopper* [5].

5 Conclusion

We have presented two types of general flat-foldable cylindrical deployable structures composed of rigid quadrilateral panels. The isotropic generalization is based on combinations of appropriate joint structures, and the anisotropic generalization is based on the folding motion of parallelogram strips. We have shown that isotropic general structures can be realized by using thick panels and hinges and anisotropic structures can be realized by using multilayered surfaces.

Acknowledgement

This research is supported by a Grant-in-Aid for JSPS Fellows funded by Japan Society for the Promotion of Science.

References

[1] Guest, S. D. and Pellegrino, S., The folding of triangulated cylinders, Part I: Geometric considerations, *ASME Journal of Applied Mechanics*, 1994, Vol.61, 773–777

[2] Hoberman, C., Reversibly expandable three-dimensional structure. United States Patent No. 4,780,344, 1988

[3] Hoberman, C., Curved pleated sheet structures. United States Patent No. 5,234,727, 1993

[4] Kuribayashi, K., Tsuchiya, K., You, Z., Tomus, D., Umemoto, M., Ito, T. and Sasaki, M., Self-deployable origami stent grafts as a biomedical application of ni-rich tini shape memory alloy foil, *Materials Science and Engineering A*, 2006, Vol.419, 131–137

[5] McNeel, grasshopper - generative modeling for rhino, `http://grasshopper.rhino3d.com/`

[6] Nojima, T., Origami modeling of functional structures based on organic patterns, 2007, Presentation Manuscript at VIPSI Tokyo `impact.kuaero.kyoto-u.ac.jp/pdf/Origami.pdf`

[7] Sogame, A. and Furuya, H., Conceptual study on cylindrical deployable space structures, In *IUTAM-IASS Symposium on Deployable Structures: Theory and Applications* (2000), pp. 383–392

[8] Wu, Z., Hagiwara, I. and Tao, X., Optimisation of crush characteristics of the cylindrical origami structure, *International Journal of Vehicle Design*, 2007, Vol.43, 66–81

[9] Yenn, T., Flip flop, `http://erikdemaine.org/thok/flipflop.html`